Life Cycle Assessment of Nitrogen Fixation Process Assisted by Plasma Technology and Incorporating Renewable Energy

Aikaterini Anastasopoulou [1], Sughosh Butala [1], Juergen Lang [2], Volker Hessel [1] , Qi Wang [1]*

[1] Laboratory of Chemical Reactor Engineering / Micro Flow Chemistry and Process Technology, Department of Chemical Engineering and Chemistry, Eindhoven University of Technology, P.O. Box 513, 5600 MB Eindhoven, The Netherlands

[2] Innovation Management, Verfahrenstechnik & Engineering, Evonik Technology & Infrastructure GmbH, Rodenbacher Chaussee 4, 63457 Hanau-Wolfgang, Germany

* Author to whom correspondence should be addressed; E-Mail: q.wang1@tue.nl;

Tel.: +31(0)402478290

1. Process Modeling and Simulation

In order to acquire the inventory data for the LCA study, both the conventional and plasma-assisted nitric acid syntheses have been simulated in ASPEN Plus software with the aid of literature data. In terms of the research studies reported so far on the ASPEN process simulations of the nitric acid synthesis, the majority of them focus mainly on the absorption of NO_x gases in water rather than the full-scale production.[1,2] Even the very few case studies that provide complete mass and energy balances of the entire process, they lack in presenting a robust process simulation model, as well as, the implemented reaction kinetics.[3] For that reason, an ASPEN model for the commercial-scale nitric acid production by both conventional and plasma-assisted technologies has been fully developed and is introduced in detail in the following sections.

1.1. Thermodynamic Models and Physical Property Methods

The integrated electrolyte NRTL and Redlich-Kwong model has been deployed from the ASPEN Plus Properties Package for the calculation of the activity coefficients of components in liquid phase and the vapor-liquid equilibria.[1,4] The components of N_2, O_2 NO, NO_2, N_2O_4, HNO_2 and HNO_3 –as will be introduced below– have been defined as Henry components. The Henry Law constants required to calculate the gas solubility have been extracted from literature.[5] The only exception is the HNO_3 component whose Henry Law constant has been estimated upon a regression analysis of experimental data embedded in the NIST databank.

1.2. NO_x Gas Reaction Set

The reaction modelling of NO_x absorption by water constitutes a complex procedure due to the fact that it involves more than 40 reactions, occurring in both gas and liquid phases, with different kinetic expressions proposed by various researchers.[1,2,4–9] In order to facilitate the execution of the proposed ASPEN model a given number of reactions in both gas and liquid phases has been selected from literature, as shown in Tables S1 and S2, with their respective kinetics.

Table S1. Gas-Phase Reactions

Reaction	Kinetic Expression	Reference
R1. $2NO + O_2 \rightarrow 2NO_2$	$\ln k_1 = \frac{530}{T} + 7.09 \; (L^2 \cdot mol^{-2} \cdot s^{-1})$	10
R2. $2NO_2 \leftrightarrow N_2O_4$	$\ln K_2 = \frac{6893}{T} - 25.865 \, (kPa^{-1})$	1
R3. $3NO_2 + H_2O \leftrightarrow 2HNO_3 + NO$	$\ln K_3 = \frac{2003.8}{T} - 10.763 \, (kPa^{-1})$	1
R4. $NO + NO_2 + H_2O \leftrightarrow 2HNO_2$	$\ln K_4 = \frac{2051.17}{T} - 8.7385 \, (kPa^{-1})$	1

Table S2. Liquid-Phase Reactions

Reaction	Kinetic Expression	Reference
R5. $2NO_2 + H_2O \rightarrow HNO_2 + HNO_3$	$\log k_5 = 4.67209 \, (m^2 \cdot mol^{-2} \cdot s^{-1})$	1
R6. $N_2O_4 + H_2O \rightarrow HNO_2 + HNO_3$	$\log k_6 = -\frac{4139}{T} + 16.3415 \, (s^{-1})$	8
R7. $3HNO_2 \rightarrow HNO_3 + H_2O + 2NO$	$\log k_7 = -\frac{6200}{T} + 20.1979 \, (atm^2 \cdot m^9 \cdot kmol^{-3} \cdot s^{-1})$	8

1.3. Conventional Nitric Acid Process

The conventional nitric acid process has been designed based on the operating conditions reported in literature with certain modifications due to the lack of coherent and verified reaction kinetics for the NO_X absorption.[3] The production capacity has been defined to 280 TPD. In the process flowsheet depicted in Figure S1, moist atmospheric air – 78% N_2 , 21% O_2 and 1% H_2O (v/v) – is compressed and split in two streams: a) a primary air stream which is directed to the reactor and b) a secondary air stream which is inserted to the bleaching column. The primary air is mixed with the superheated ammonia stream and the feed is further inserted in the ammonia oxidation converter. The reactor has been modelled by a stoichiometric reactor operating at 11 bar and 645°C and employing the following reaction set with the corresponding ammonia conversion values:

$$4NH_3 + 5O_2 \rightarrow 4NO + 6H_2O \text{ (R8) [95\%]}$$

$$2NH_3 + 3O_2 \rightarrow 2N_2 + 6H_2O \text{ (R9) [4\%]}$$

$$4NH_3 + 4O_2 \rightarrow 2N_2O + 6H_2O \text{ (R10) [1\%]}$$

The generated NO gas stream is cooled down through a system of five heat exchangers from 645°C to 65°C. The first three heat exchangers –HX2, HX3 and HX4– have been simulated by plug flow reactors employing the reaction and kinetics of R1 from Table S1. The design parameters of the plug flow reactors have been such selected that 5%, 18% and 32% (w.w.) oxidation of nitric oxide to nitric dioxide is achieved, respectively. The condenser of the system is simulated by a system of two plug flow and one CSTR reactors so as to facilitate both the nitric oxide oxidation and the nitric acid formation. The plug flow reactors have been such designed that 42% oxidation of NO to NO_2 is obtained. The CSTR reactor employing the reactions R3, R5 and R6 of Table S1 and Table S2, serves as a condenser generating a 40% weak acid which is inserted on the 13th tray of the absorption column. Prior to the final heat exchanger of the cooling system, the reaction gas exiting the condenser is mixed in a reactor pressure vessel –oxidation unit– with the tail gas of the bleaching column where further NO oxidation occurs at temperature of 140°C. The reaction gas stream leaving the oxidation unit is cooled down through the HX5 and oxidized to nitric dioxide and dinitrogen tetroxide. The given heat exchanger has been simulated with a plug flow and a CSTR reactor, the first one accommodating the oxidation of NO and the latter one the N_2O_4 formation. Design specifications have been selected such that the mass percent composition of the nitrogen oxides in the final NO_x gas stream is, approximately, 70% NO_2, 27% N_2O_4 and 3% NO. The gas stream is directed thereafter to the bottom tray of the absorption column where further nitric acid is formed.

The absorption column has been simulated by an equilibrium RadFrac block in ASPEN. It has been modelled with 59 sieve trays of 0.5 m spacing and diameter of 1.8 m. The reactions R1– R7, as presented in Table S1 and S2, have been specified to take place at all stages with a liquid and gas residence time of 15 seconds. The operating pressure has been set to 10 bar. Deionized water stream is inserted on the top tray of the absorption column at 7°C, whereas the weak HNO_3 and NO_X gas stream (approximately 11 % w.w. NO_x) is fed on the 13^{th} and 59^{th} bottom tray, respectively. Due to the exothermic reactions occurring in the absorption column, there is a need of external cooling system that will enable the outlet temperature of the tail gas to be below 20°C. The cooling requirements of the column are covered by an external cooling water stream with the form of a pump-around from the bottom to the top tray instead of external coolers allocated to each stage. The tail gas exits the top tray of the absorption column at 19°C. The formed weak HNO_3 solution of 60% w.w. is then leaving the bottom tray and is entering the bleaching column for further removal of NO_x traces.

The bleaching column is simulated by an equilibrium RadFrac unit with 20 stages and an operating pressure of 10 bar. The weak HNO_3 stream is inserted on the 1st tray, whereas a secondary air stream is directed to the 20th tray. By this process approximately 99% of the NO_x gas dissolved in the initial HNO_3 stream is practically removed. The outlet temperature is determined to

53°C and 67°C for the gas stream (tail gas-1) and the produced weak HNO_3 solution, correspondingly.

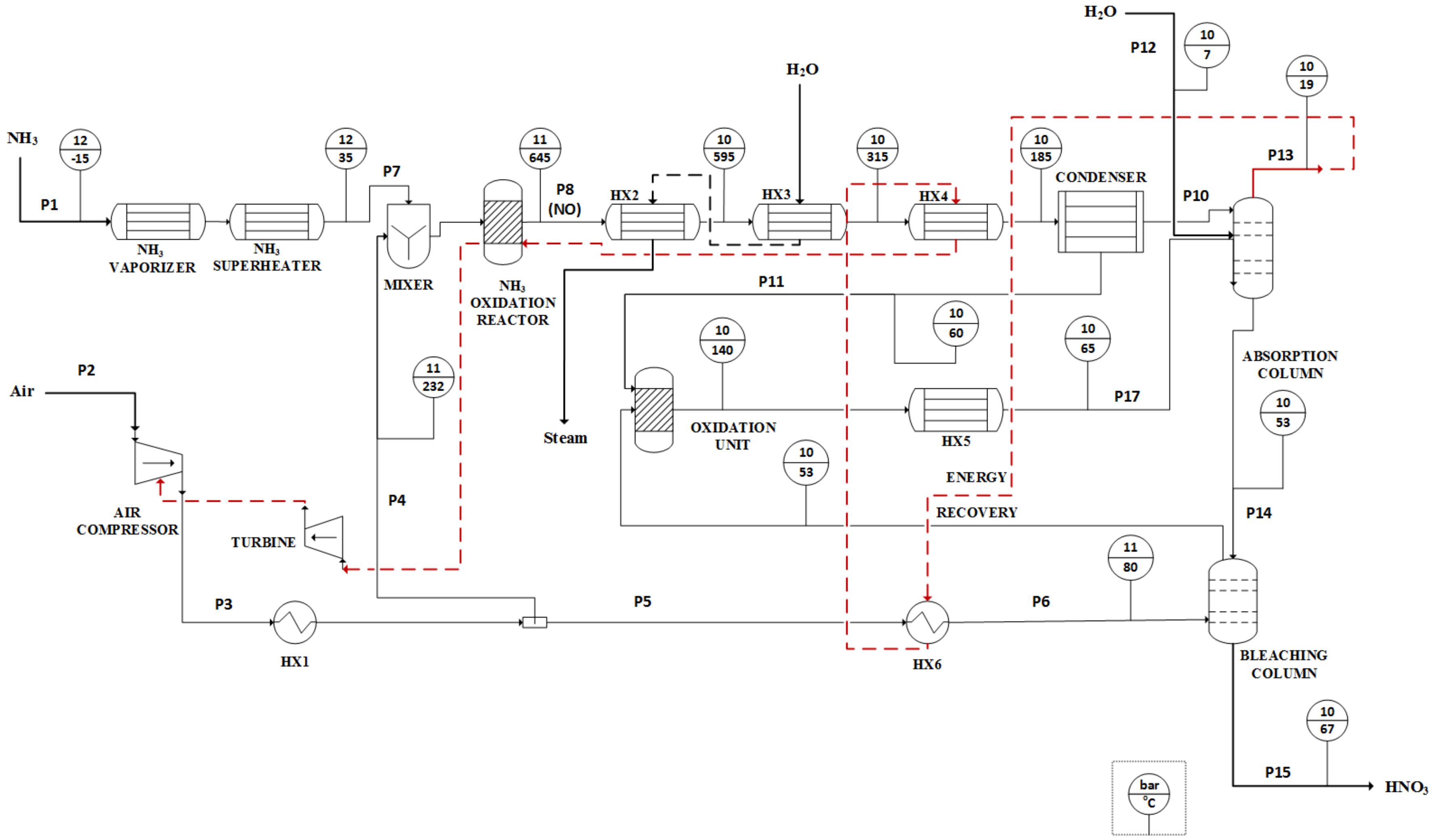

Figure S1. Process flow-sheet of conventional HNO$_3$ synthesis

1.4. Plasma-assisted Nitric Acid Process

In terms of the process modelling of the plasma-assisted nitric acid production, a base case scenario for a production capacity of 10TPD has been developed so as to facilitate the conceptual design of a modular mini plant. Dry atmospheric air –79% N_2 and 21% O_2 (v/v)– and pure O_2 stream (90% purity) with a volumetric flow ratio N_2/O_2 of 1.86:1 have been selected as a feed for the plasma reactor. PSA technology has been selected for the O_2 generation. The air flow requirements for the PSA unit, and in turn O_2 mass flow, has been determined by the selected NO molar yield of 6% –as it will be further explained in the section of the plasma reactor design– based on given technical reports[11]. The air stream is compressed to 7 bar and cooled down to 20°C prior to its entrance in the PSA-O_2 unit. The air stream compressed for the PSA-O_2 units is split to two streams, one primary for the pure O_2 generation and a secondary for the bleaching column.

The plasma reactor employed for the NO synthesis is a Gliding Arc reactor operating at ambient conditions. Considering the complexity of the plasma process, as well as, the limitation of ASPEN Plus software in terms of complicated process simulations, the reactor has been modelled by a stoichiometric reactor with an outlet gas temperature of 100°C, as shown in Figure S2. Regarding the yield of fixed nitrogen –including NO, NO_2, N_2O_4 etc.– reported in literature for a N_2/O_2 system, various values have been proposed for different plasma technologies ranging from 1 to 20% [12]. However, in the present case study the assumption of standalone NO synthesis and the selected molar yield of 6% for 1.86:1 N_2/O_2 feed have been considered. The power consumption of the plasma reactor has been defined to 7.7 kWh/kg NO based on literature for the given NO yield [13]. Under these operating conditions, the generated NO gas stream is compressed to 6 bar so as to facilitate the NO_X absorption occurring at a later stage.

After the compression step, the NO reaction gas is cooled down through a system of two heat exchangers at temperature of 60° C. As the NO gas runs through the piping and the heat exchanger is oxidized to NO_2 which, in turn, is dimerized to N_2O_4. In order to simulate the particular reaction system in ASPEN, a plug flow reactor incorporating the NO oxidation reaction and a CSTR reactor for the NO_2 dimerization reaction has been assumed in place of the heat exchangers being realized in the preliminary process design. The design specifications of the plug flow reactor have been selected for an operating pressure of 6 bar and a desired NO oxidative conversion of 90%, as proposed by literature for the conventional route[8]. The reaction gas stream from the plug flow reactor is, then, driven to the CSTR operating at the same pressure with a chosen reaction residence time of 6 seconds. After this step, the generated NO_x gases are mixed with the tail gas from the bleaching column (tail gas-1) and the resulted stream (approximately 9% w.w. NO_x) is directed to the bottom tray of the absorption column.

The simulation of the absorption and bleaching columns follow the same concept as that of the conventional process, as presented above, with few modifications. In this case, the absorption column has been modelled for an operating pressure of 6 bar with 10 sieve trays of 0.25 m. spacing and a diameter of 0.6 m. The liquid and gas residence time is specified to 20 seconds and the outlet tail gas temperature is defined to 20°C. Additionally, the bleaching column is simulated with 5 stages and the same pressure as the absorption tower. The temperature of the outlet NO_x gas and weak HNO_3 solution streams is determined to 50°C and 45°C, respectively.

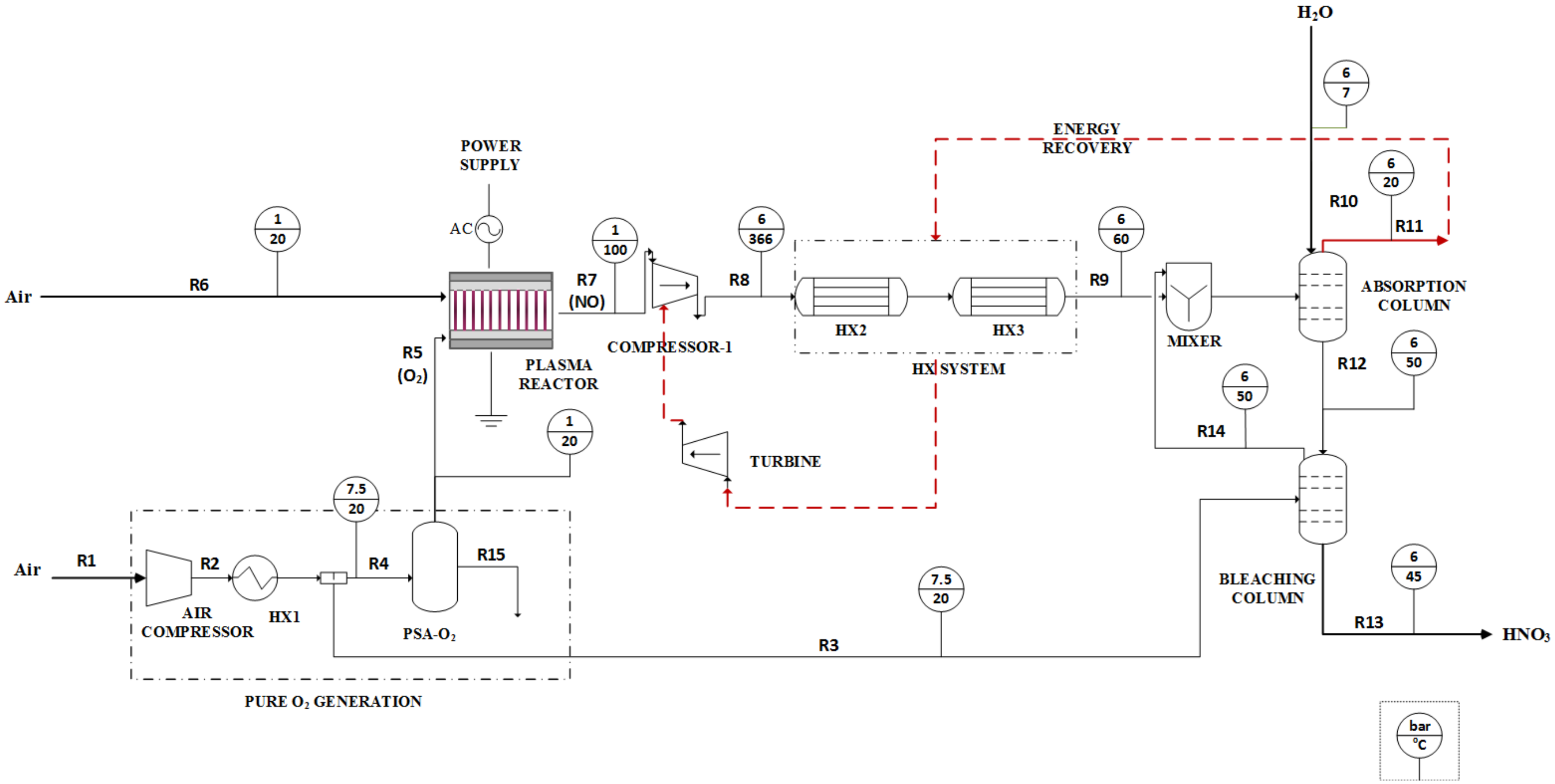

Figure S2. Process flow-sheet of plasma-assisted HNO_3 synthesis

1.5. Energy Considerations

The conventional nitric acid synthesis is an energy efficient process since it covers the majority of its energy requirements by the recycle of the tail gas stream and part of the generated superheated steam. In specific, the tail gas of the absorption column passes through the HX6, HX4 and the ammonia oxidation unit for an enhanced energy recovery, as shown in Figure S1. Due to the high outlet temperature, the tail gas is expanded in a turbine for power production driving partially the air compressor. Apart from the tail gas expansion, superheated steam is generated by the heat duty of the HX2 and HX3, part of which is utilized for covering the remaining power requirements of the air compressor. The energy requirements of the ammonia vaporizer and HX5 are covered by a warm water loop whereas the heating requirements of the ammonia superheater are also covered by the generated steam.[3] Considering the aforementioned, the heat and power needs of the particular process equipment are not reflected as energy input in the system boundaries of the conventional nitric acid synthesis.

With respect to the process simulations of the plasma-assisted nitric acid synthesis, a parametric analysis has been conducted in order to evaluate the respective environmental footprint and, in turn, provide the preferable –from an ecological viewpoint– operating regime for the studied chemical process. More specifically, within the scope of this research study the effect of four critical operating parameters on the overall mass and energy profile of the plasma process has been assessed. The selected parameters are: a) the plasma-assisted NO yield b) the power consumption of the plasma reactor c) the recycle of the tail gas stream and d) the energy recovery scheme in the case of thermal plasma reactor. Detailed design considerations and assumptions employed in each parametric scenario are provided below.

a) NO yield scenario

Taking into account the lack of reported literature data on the correlation between power consumption and NO yield in either thermal or non-thermal plasmas, for the particular scenario two arbitrary values of NO molar yield, 2% and 10%, have been selected and simulated for the same production capacity, power consumption of the plasma reactor and operating conditions presented for the base case scenario. This selection, though arbitrary, has been made based on the limitation of the plasma NO synthesis in achieving high product yield as compared to conventional process. However, contemporary technology advancements have yielded new insights in plasma chemistry and, thus, an improvement in the NO yield is also likely to be reported in the near future.

Similar to the latter process, an energy recovery approach has also been adopted for the plasma-assisted nitric acid synthesis. More precisely, based on the ASPEN simulations, the feasibility of utilizing the tail gas as a cooling and power generation mean for the heat exchanger system and the compressor, respectively, has been tested through a pinch analysis study. Energy savings from the use of tail gas are presented in Table S3, for both the conventional and the different NO yield scenarios.

Table S3. Percentage of cooling and electricity savings from the tail gas heat recovery

	Conventional Process	Plasma-assisted Process		
		2% NO	6% NO	10% NO
Cooling Energy Savings	30%	34%	31%	26%
Electricity Savings	80%	24%	24%	22%

The percentage profile of the cooling and electricity savings for the studied NO yield scenarios depicted in Table S3 cannot be easily interpreted on the basis of a certain trend. The reason behind this lies in the fact that the energy recovery scheme-heat recovery by passing the tail gas through the HX system and electricity generation by the tail gas expansion- is affected by both cooling requirements of the HX system and the concentration of the tail gas. As long as these two parameters change in all the studied NO yield scenarios, the overall impact on the final cooling and electricity savings can either same or different, like the cases of 2% and 6% NO yield which present an equivalent percentage of electricity savings.

b) Plasma power consumption scenario

In terms of the plasma power consumption scenario, based on literature data the value of 33.3 kWh/kg NO for 6% NO yield have been considered and evaluated along with the base case scenario[13]. Although this energy value refers to different plasma technologies from the Gliding arc reactor employed in the present research work, its use facilitates, alike the NO yield scenario, the sensitivity analysis deployed in the LCA.

c) Tail gas recycle scenario

The particular scenario considers the recycle of the tail gas stream to the plasma reactor after the implementation of the energy recovery scheme presented in the Figure S2. The operating and design parameters are considered the same as for the base case scenario.

d) Energy Recovery Scenario

In the case of non-thermal plasma technology, which has been considered as an applied technique in the current research study, the energy efficiency is relatively low since the majority of the power input is utilized to dissociate electrons rather than heating the rest gas particles. This, in turn, results to low background gas temperatures and any energy recovery potential is basically hindered. However, on the other hand, thermal plasmas are characterized by high background gas temperatures reaching up to 10^4 Kelvin which enables enhanced heat recovery and overall energy efficiency.

In order to provide an insight on the environmental performance of the plasma-assisted nitric acid synthesis incorporating an energy recovery scheme, a certain process design scenario has been developed. Based on the same operating conditions given for the tail gas recycle scenario, the following assumptions have been also considered: a) heat losses from the plasma reactor are negligible and b) the input energy of the plasma reactor is merely utilized in the formation of the NO molecules –with $\Delta_f H^o = 90.29$ kJ/mol– and the increase of the gas temperature from 20 to 100^oC. Upon these considerations, the remaining energy is recovered in the form of generated steam. Although, this scenario may be perceived as optimal and further design considerations need to be incorporated, it serves, at this stage, the aim of the present LCA study for a preliminary assessment of different plasma process operating conditions and design alternatives towards the nitric oxide, and in turn to nitric acid, synthesis against the conventional production route.

2. Inventory Data Analysis

Table S4. Description of activity datasets from Ecoinvent 3.0 employed in the LCA study

Ecoinvent 3.0 – Activity Dataset	Description
• ammonia production, steam reforming, liquid [RER]	From cradle, i.e. including all upstream activities. Manufacturing process starting with natural gas, air and electricity is considered, plus auxiliaries, energy, transportation, infrastructure and land use, as well as wastes and emissions into air and water. Transport of the raw materials, auxiliaries and wastes is included, transport and storage of the product are not included. Carbon Dioxide is the byproduct generated. Transcient or unstable operations are not considered, but the production during stable operation conditions. Emissions to air are considered as emanating in a high population density area. Emissions into water are

	assumed to be emitted into rivers. Values are taken principally from EFMA 2000 and Frischknecht 1999 (see report). Inventory refers to 1 kg 100% ammonia, liquid, at plant.
• cooling energy, from natural gas, at cogen unit with absorption chiller 100kW [CH]	From cradle, i.e. including all upstream activities. The module includes heat input from a 160kWel cogeneration unit, electricity and water needed for operation and infrastructure (absorption chiller, air cooler, piping). The module reflects an absorption chiller operated with heat from a natural gas operated cogeneration unit (allocation exergy). Life time for the total system assumed with 20 years or 20'000 full operating hours.
• compressed air production, 1000 kPa gauge, <30kW, average generation [RER]	From cradle, i.e. including all upstream activities. This dataset includes the compressor, operating materials (lubricating oil), the electricity consumption as well as the transports of the compressor and the lubricant to the installation site. The material for the supply and the energy needed to hold the pressure in the supply installation is included. The installation at the site is not included. The distribution network (from the compressor to the final consumer) is part of this dataset. This network cannot be separated since the pressure in the network is maintained by the compressor which is part of the transforming activity. Two types of network are introduced (based on research presented in ecoinvent report 23_MechanicalEngineering); small installations with compressor capacity below 30kW and large installations with compressor capacity above 30kW. This dataset includes small installation (<30kW).
• steam production in chemical industry [RER]:in MJ	Activity starting with the input of heat and electricity mix From cradle, i.e. including all upstream activities. Activity ends with the production of 1 MJ heat (=0.3636 kg) steam

	from cold water. Does not include the water input because steam is often used in closed systems. This inventory is to be used for heat energy production in average chemical plant, in case no information is available about the source of the heat energy. It represents the fuel mix of the average steam production in the chemical industry. The data are arithmetic average of all 215 steam plants. The energy content of the steam is 2.75 MJ/kg which corresponds to an overall efficiency of 74%.
• water production, deionised, from tap water, at user [RoW]	From cradle, i.e. including all upstream activities. Energy for operation, chemicals used for regeneration, transport of chemicals to plant, emissions from regeneration chemicals, infrastructure of plant and replacement of spent exchane resin. Process does not include very small units (cartridges) or very large units with >>100 m3/h (power stations). Other production methods as reverse osmosis electrodialysis or distillation are not covered with this process (only ion exchange).
• compressed air production, 800 kPa gauge, >30kW, average generation [RER]	From cradle, i.e. including all upstream activities. This dataset includes the compressor, operating materials (lubricating oil), the electricity consumption as well as the transports of the compressor and the lubricant to the installation site. The material for the supply and the energy needed to hold the pressure in the supply installation is included. The installation at the site is not included.
• electricity production, natural gas, at conventional power plant [DE]	From cradle, i.e. including all upstream activities. The module includes fuel input from high pressure (DE) network, infrastructure, emissions to air, and substances needed for operation.
• electricity production, photovoltaic,	From the PV module installed and ready to

570kWp open ground installation, multi-Si [DE]	be used. From cradle, i.e. including all upstream activities. This activity ends with low voltage electricity produced with the 570 kWp module, assuming an average yield. This dataset includes tap water use for cleaning the module and its treatment. This dataset represents the production of grid-connected low voltage electricity with a 570 kWp open ground photovoltaic (PV) plant in Germany in 2008. Large central photovoltaic power stations in the higher kilowatt to megawatt range can feed directly into the medium- or high voltage grid. However, the voltage depends largely on the design and size of the plant. In order to treat all photovoltaic installations the same way (no matter which size, design and installation type (building integrated or open ground)), low voltage electricity is assumed as a product in this dataset. The plant consists out of multi-Si panel modules with a total capacity of 570 kWp. An inverter is used to convert the low voltage DC power into AC power. An average yield of 950 kWh/kWp was assumed for the calculations.
• electricity production, wind, 1-3MW turbine, offshore [DE]	From (kinetic) wind energy, entering the power plant. From cradle, i.e. including all upstream activities. This activitiy ends with 1 kWh of produced electricity at the power plant. The dataset includes lubricating oil from maintenance of the installation. The dataset doesn't include the land use as shipping is assumed to be restricted to a small extent. This dataset represents the production of 1 kWh electricity from wind power in one specific (2 MW) offshore wind power plant
• electricity production, lignite [DE]	From cradle, i.e. including all upstream activities. Energy conversion for electricity production. Particle removal is included in this module. DeSOx and DeNOx are described

	in different modules; they are applied here according to the actual use in the country; SOx and NOx emissions are the reduced ones. It is assumed that 25 % of the plants are river cooled, 75 % use cooling tower (average UCTE). The water treatment is described in separate modules. The disposal of non-recycled ashes is modelled separately. The module describes the average for the country. The plant is used for middle load with 6000 hours of operation at full capacity per year. The plant is assumed to operate 200000 hours during its lifetime.
• electricity production, hydro, run-of-river [DE]	From (potential) energy in water, entering the power plant. From cradle, i.e. including all upstream activities. The activity ends with 1 kWh of high voltage electricity produced at the power plant and arrived at the busbar. The datasets includes the use of lubricant oil and the mass of water assing through the turbines. The dataset doesn´t include detailed specifications about land use due to methodical issues. This information is only included via transformation and occuption of land and calculated with a simplified approach. This dataset represents the production of 1 kWh of electricity in a run-of-river power plant unit in Germany in 2008.

3. Results and Discussion

Table S5. Absolute values of selected impact factors for both processes (per ton HNO_3 (60% w.w.))

Impact factor	**Unit**	**Plasma-assisted nitric acid process**					**Conventional nitric acid process**
		Wind energy	***Solar energy***	***Hydroelectric energy***	***Lignite***	***Natural gas***	
Acidification potential (AP)	kg SO_2-Eq	1.68	3.72	1.38	6.37	4.82	1.51
Global warming potential (GWP)	kg CO_2-Eq	529.34	796.80	478.97	5399.89	2795.10	620.97
Eutrophication potential (EP)	kg NO_x-Eq	1.23	2.14	1.09	5.43	3.30	0.92
Human toxicity potential (HTP)	kg 1,4-DCB-Eq	399.11	520.73	178.48	415.54	373.64	298.30
Marine aquatic ecotoxicity potential (MAETP)	kg 1,4-DCB-Eq	1236.84	1823.42	482.64	22111.18	830.37	621.68
Photochemical oxidant creation potential (POCP)	kg ethylene-Eq	9.76E-02	1.94E-01	7.86E-02	0.26	0.32	8.69E-02
Ozone depleting potential (ODP)	kg CFC-11-Eq	9.97E-05	2.03E-04	9.65E-05	1.26E-04	7.99E-04	1.34E-04
Cumulative fossil energy demand (CED)	MJ-Eq	7974.27	11264.05	7426.98	58586.86	48346.68	9695.32

The Table S5 shows the absolute values of all the environmental impact factors tested in this base case scenario for both conventional and renewable electricity systems. As it can be inferred, non-renewable energy utilization manifests a poor profile for almost all LCA emission factors as compared to conventional process. To exemplify, the AP values of the lignite and natural gas electricity scenarios are 4 and 3 times higher than the corresponding value of conventional nitric acid production, respectively. An increase is also displayed for the HTP values of the aforementioned energy sources reaching up to 39% and 25%, correspondingly. Albeit the meager improvement in the ODP of the lignite energy, the standalone fossil fuel power systems are proven inferior to the conventional process with respect to their overall impact factors profile.

It can also be concluded from Table S5 that the employment of renewable energy sources, such as solar, hydroelectric and wind energy, enhances the overall environmental performance of the plasma-assisted nitric acid synthesis with respect to certain impact factors. More precisely, for the cases of wind and solar energy a considerable decrease in AP is observed by 65% and 23%, respectively, as to that of standalone natural gas. In addition to that, CED –an important process performance indicator– is reduced by 84% and 77%, correspondingly.

For the given process design conditions, renewable energy sources demonstrate generally a more moderate environmental performance as to the conventional nitric acid production with some impact factors being either lower or higher. The MAETP and CED of wind energy can serve as descriptive example of this trend with their values being 99% higher and 18% lower than those of conventional process, respectively. Only, the hydroelectric power system exhibits a clear environmental leverage over the benchmark case study with respect to all the LCA impact factors. In specific, both AP and GWP are improved by 9% and 23% as compared to the conventional one.

References

(1) Hüpen, B.; Kenig, E. Y. Rigorous modelling of NO x absorption in tray and packed columns. *Chem. Eng. Sci.* **2005**, *60*, 6462–6471.

(2) Suchak, N. J.; Jethani, K. R.; Joshi, J. B. Modeling and simulation of NOX absorption in pilot-scale packed columns. *AIChE J.* **1991**, *37* (3), 323–339.

(3) Ray, M. S.; Johnston, D. W. *Chemical Engineering Design Project: A Case Study Approach*, 2nd ed.; CRC Press, 1998; pp 1–360.

(4) Spoor, M. Modeling and stochastic simulation of the reactions and absorption of NOx in water, Delft University of Technology, 1992.

(5) Schmidt, D. D. Simulating Aerosol Formation and Efefcts in NOx Absorption in Oxy-fired Boiler Gas Processing Units Using ASPEN Plus, Kansas State University, 2013, pp 1–76.

(6) Miller, D. N. Mass transfer in nitric acid absorption. *AIChE J.* **1987**, *33* (8), 1351–1358.

(7) Wiegand, K. W.; Scheibler, E.; Thiemann, M. Computation of plate columns for NOx absorption by a new stage-to-stage method. *Chem. Eng. Technol.* **1990**, *13* (1), 289–297.

(8) Thiemann, M.; Sceibler, E.; Wiegand, K. W. Nitric Acid , Nitrous Acid , and Nitrogen Oxides. *Ullmann's Encyclopedia of Industrial Chemistry*; 2012; pp 177–225.

(9) Joshi, J. B.; Mahajani, V. V.; Juvekar, V. A. *Invited Review Absorption of NOx Gases*; 1985; Vol. 33, pp 1–92.

(10) Tsukahara, H.; Ishida, T.; Mayumi, M. Gas-Phase Oxidation of Nitric Oxide : Chemical Kinetics and Rate Constant. *NITRIC OXIDE Biol. Chem.* **1999**, *3* (3), 191–198.

(11) Copco, A. Atlas Copco PSA Oxygen Generators http://www.atlascopco.com/nitrogenus/system/splash.aspx.

(12) Patil, B. S.; Wang, Q.; Hessel, V.; Lang, J. Plasma N2-fixation: 1900–2014. *Catal. Today* **2015**, *256*, 49–66.

(13) Mutel, B.; Dessaux, O.; Goudmand, P. Energy cost improvement of the nitrogen oxides synthesis in a low pressure plasma. *Rev. Phys. Appl.* **1984**, *19*, 461–464.